ADDIS ABABA UNVERSITY

SCHOOL OF GRADUATE STUDIES

MEASURING THE ELECTRICAL PROPERTY AND INFRARED LIGHT SENSITIVITY OF PREIONIZED 24 HOURLY TREATED BREAST CANCER CELLS USING LASER TRAPPING TECHNIQUES

BY:

YETWALE ALEMU

ATHESIS SUBMITTED TO THE DEPARTMENT OF PHYSICS IN PARTIAL FULFILMENT OF THE REQUREMENTS FOR THE DGREE OF MASTER OF SCINCE IN LASER PHYSICS.

ADDIS ABABA UNVERSITY

September 2023

APPROVAL SHEET OF THESIS

Addis Ababa University

School of graduate studies

As a member of the examining board for the finale MSc open defense, we certify that we have read and evaluated the thesis prepared by Yetwale Alemu.

Entitled: Measuring the electrical property and infrared light sensitivity of pre ionized 24 hour treated breast cancer cells using laser trapping techniques re**c**ommended that it be accepted as fulfilling the thesis requirement for the degree of Master of Science in Laser Physics. It complies with the regulation of university rules and meets the accepted standards with respect to originality and quality.

Submitted by Yetwale Alemu signature ----------date ----------

Advisor Endries Muhammed (PH.D) signature ----------date ----------

Approved by the examination committee

Name ----------signature----------date ----------

(Chairman)

Name ----------signature ----------date ----------

(Internal examiner)

Name ----------signature----------date ----------

(External examiner)

Final approval and acceptance of the thesis is dependent on the submission of the final copy of the thesis to the Council of Graduate Studies through the School of Graduate Studies Graduate Committee of the candidate's major department.

Addis Ababa University

Date ----------

Author: YETWALE ALEMU

Title: Measuring the electrical property and infrared light sensitivity of pre ionized 24 hour treated breast cancer cells using laser trapping techniques.

Department: physics

Degree: MSc convocation ----- 2023

September, 2023

ADDIS ABABA, ETHIOPIA

STATEMENT OF THE AUTHORS OF THE THESIS

The author's statement

I hereby affirm that this thesis is entirely my original work, and I have duly acknowledged all sources used in its preparation. This thesis is submitted as part of the requirements for obtaining MSc degree in laser physics from Addis Ababa University. It has been deposited in the university library and is available for borrowing in accordance with the library's regulations.

I solemnly declare that this thesis has not been submitted to any other academic institution, anywhere, for the purpose of obtaining any academic degree, diploma, or certificate. Permission is granted for brief quotations from this thesis, provided that proper acknowledgment of the source is made. Requests for extended use or reproduction of this manuscript, whether in full or in part, may be considered by the head of the relevant department or the head of the school of graduate studies if it is deemed to serve scholarly purposes. In all other cases, permission must be sought directly from the author.

Name ---------- sign ----------

Place --- Addis Ababa University.

Date of submission ----------

ACKNOWLEDGEMENTS

First, I would like to thank the almighty God for helping me throughout my life. Then, I would like to express my gratitude to my instructor, Endris Mohammed (PH.D), for his consistent advice, supervision, suggestions, friendly encouragement, proofreading my thesis, giving me valuable comments, and brother hood approach to my work as wells provided the 4T1 breast cancer cells that were grown and extracted from Tennessee Center for Botanical Medicine Research's International Ginseng Institute for the investigation. This work would have not been possible without the sponsorship of ministry of education of Ethiopia, Amhara educational bureau. Next, I am highly beholden to my wife Amelework Badimaw and my son Nathan Yetwale, who paid better scarification to be successful me, to develop me, and to teach me. I would like to extend my thanks to my fellow students, Gedefaw Ayaliew, Nugussu Birhanu, Kerebh Chanie, and Guta, for their unlimited support and advice. In addition, I would like to thank Durbete high School and my student Murad Achene, for their support in getting internet access and material support. Lastly, I would like to thank my country, Ethiopia, and Addis Ababa University, as well as the physics department, for their facilitation and knowledge streams for the MSc.

TABLE OF CONTENTS

TABLE OF FIGURE

TABLE OF TABLES

ABSTRACT

A study was conducted to introduce a novel method utilizing laser trapping techniques for measuring the electric charge and coefficient of the laser trap for breast cancer cells treated continuously for 24 hours. The 4T1 breast cancer cells used in this study were treated with a compound called 2-Dodecyl-6-methaxycyclohexa-2, 5-diene-1, 4-dione (DMDD). A high-power infrared laser operating at 1064nm was utilized to trap individual 4T1 cells from the group treated continuously for 24 hours. The measured values for the spring constant (k) ranged from 0.05 µN/m to 1.11 µN/m, with an average value of 0.38 µN/m. The data showed a high correlation, as indicated by an R-square value of 0.98. The charge developed on each of the 24-hourly treated breast cancer cells was quantified relative to the charge of an electron. On average, the cells exhibited a charge of -2249.55 ± 1983.89 units. It was observed that the charge developed on the cell surface was influenced by the size of the cells. As the cells moved closer to the laser trap, their charge increased, while their velocity, acceleration, and momentum decreased. After determining the electrostatic force and trapping force, a homogeneous second-order differential equation was solved to further analyze the system. This study provides valuable insights into the relationship between charge development, spring constant, and cell size in continuously treated breast cancer cells using laser trapping techniques. Velocity and acceleration decreases as the cells approaches to the trap and spring constant and mass have positive correlation to the charge developed on the cells

CHAPTER ONE

1. INTRODUCTION

Laser, an acronym highlighting a key aspect of its functioning, is instrumental in amplifying light through radiation stimulation. Every laser device designed to amplify radiation contains essential components. These components include a material capable of radiation amplification, often referred to as the gain medium [1]. The notion of transmitting laser energy through space has been proposed, achieved by applying stimulated energy to a lasing medium. This radiation energy, falling within the visible or infrared spectrum, is termed radiation energy. The medical application of lasers dates back to 1963 when ophthalmologists first explored their use. Presently, lasers find widespread use in medical procedures, including the treatment of cancer through laser therapy [2]. Cancer, a leading cause of global mortality, remains a significant concern across both developing and developed nations. According to the International Agency for Research on Cancer (IARC), nearly 2.1 million new cases of breast cancer arise annually, causing around 0.5 million deaths [3]. This study primarily centers on breast cancer cells, particularly the type that predominantly affects females. In regions with high cancer incidence, such as Europe and the USA, breast cancer ranks as the most prevalent form among women. Roughly one in ten women in the UK and USA may develop this illness during their lifetimes, making it a prominent cause of death among women in industrialized nations. Typically, breast cancer rates peak within the 50–60 age range [4].Recent advancements in cancer treatment aim to identify effective and less risky alternatives to traditional approaches, as the current methods often lead to adverse tissue effects. Various techniques are now used to treat breast cancer, encompassing surgery, radiotherapy, chemotherapy, targeted therapy, hormone therapy, radiation therapy, photodynamic therapy, and photo thermal therapy [5]. Among these, radiation therapy stands out as a precise and efficient treatment for cancers with limited metastases. Utilizing high-energy radiation such as x-rays, gamma rays, and charged particles, this approach delivers targeted treatment [6]. Another effective option for diverse malignant tumors is radiotherapy, which employs radiation energy surpassing the energy required to bind an electron. This destroys all cancer cells within a tumor. However, the unintended consequence is potential harm to the surrounding healthy cells. Hence, the focus of radiotherapy lies in intensifying radiation damage to cancer cells while minimizing harm to normal cells. Combining multiple

modalities in treatment, such as radiation and chemotherapy, is preferred over radiotherapy alone. This combined approach accelerates tumor cell death by impairing DNA repair mechanisms, and these outcomes align with laser therapy. A significant breakthrough in the 20th century, laser trapping (LT) techniques, emerged in the early 2000s. This novel optical technique, recognized by the Nobel Prize in Physics in 2018 [7], was pioneered by Ashkin. Employing the infrared laser trap at high power, the electrical properties of breast cancer cells treated over 24 hours were measured. In conclusion, lasers play a pivotal role in amplifying radiation, finding extensive use in medical applications such as cancer treatment. Breast cancer, a major concern among women globally, has led to a variety of treatment techniques, with a focus on minimizing side effects. Among these methods, radiation therapy and radiotherapy stand out, with an increasing emphasis on combination therapies. Laser trapping techniques, a remarkable advancement, have further enriched our understanding of cancer cell properties and behaviors.

1.1 Objective of the study

In this part, we will discuss the specific and general objectives of the study.

1.1.1 General objective of the study

Measuring the electrical property and infrared light sensitivity of pre ionized 24 hour treated breast cancer cells using laser trapping techniques

1.1.2 The specific objective of the study

1. Using Newtonian mechanics, the charge developed on the pre-ionized of a single 24 hr treated breast cancer cell was measured.
2. To measure the laser trap stiffness of the pre-ionized, 24-hour-treated breast cancer cells.
3. To develop a theoretical model of the equation of motion of pre-ionized breast cancer cells when the cells moving to the trap.

1.2 Outline of the thesis

The electrical properties of cancer cells and the background of cell biology with or without an external electric field were discussed in chapter two. The experimental methods for cell cultivated and treatment, the experimental arrangement, and methods of breakdown cell membrane can also be explained in Chapter 3. In chapter four, the pre-ionization of 24-hour-treated breast cancer cells are discussed. In chapter five, the results of the study can be summarized and concluded.

CHAPTER TWO

2. Back ground of the study and Literature review

In this chapter, we focus on the interactions between electric fields and near-infrared lasers interact with biological cells.

2.1 General back ground

2.2.1 Ordinary human cell

Cells are the basis of life. Like humans, individual cells within our bodies have the ability to grow, reproduce, acquire information, react to stimuli, and engage in a variety of chemical interactions. This ability defines life. There are billions or trillions of cells in ourselves and other multicellular organisms, and they are arranged into a complex structure. However, most organisms are made up of just one cell. Even Simple, unicellular organisms display all the essential characteristics of life, indicating that the cell is the basic unit of life [8]. Signals are continually influencing normal cells to determining whether to divide, develop into another cell, or die. In addition to performing several functions including giving vitamins, minerals, carbohydrates, fats, amino acids, and other nutrients, they also contain a set of rules. Nucleons, a single nucleus, and a lot of cytoplasm are present. Each mature cell performs a certain role. They are not influence anything, have fewer genetic alterations and changes, maintain normal metabolic rates, and reproduce at a controlled rate [9].

2.2.2 Cancer cell

Cancer stands as the leading cause of global mortality. Recent estimates from the International Agency for Research on Cancer (IARC) indicate that approximately 7.6 million deaths occur annually worldwide due to cancer, with a reported 12.7 million new cases emerging. The burden of this disease disproportionately affects developing nations, responsible for 63 percent of cancer-related deaths [10]. Characterized by uncontrolled and abnormal cell division, cancer often displays invasive traits. Key features include unchecked cellular proliferation, loss of differentiation, angiogenesis, metastasis, and constant interaction between proliferating cells and their surrounding stromal microenvironment [11]. Across the globe, a multitude of cancer types exists. In the United States, common cancer diagnoses exclude non-melanoma skin cancers and encompass bladder cancer, breast cancer, colon and rectal cancer, and endometrial cancer .Additionally, kidney cancer, leukemia, liver cancer, lung cancer, melanoma, non-Hodgkin

lymphoma, pancreatic cancer, prostate cancer, and thyroid cancer contribute to the spectrum of malignancies. The National Cancer Institute and other sources provide incidence and mortality data. To be classified as a common cancer, a cancer type must have a projected annual incidence of at least 40,000 cases in 2022. Leading the list is breast cancer, with an anticipated 290,560 new cases in the US in 2022[12].

2.2.3 Breast cancer

Breast cancer is a diverse group of diseases characterized by abnormal and uncontrolled growth of cells within the breast tissue. This growth pattern deviates from the normal cellular behavior and often results in the formation of a tumor or mass. The origin of most breast cancers is in the milk-producing glands known as lobules or in the ducts that connect these glands to the nipple [13]. It's important to note that while breast cancer predominantly affects females, it can also occur, albeit rarely, in males. The spread of breast cancer occurs through a process called metastasis, where cancerous cells detach from the primary tumor and enter the bloodstream or lymphatic system. The lymphatic system is a network of vessels responsible for draining excess fluids, waste products, and immune cells from tissues. This system plays a crucial role in maintaining fluid balance and immune function throughout the body. Lymphatic vessels consist of transparent fluid called lymph, which contains immune cells, cellular debris, and tissue byproducts. In the context of breast cancer, malignant cells have the ability to invade the lymphatic channels and establish growth in the lymph nodes. Many of the lymphatic vessels from the breast drain into lymph nodes located under the arm, around the collarbone, and within the chest, close to the breast bone [14]. The presence of cancer cells in these lymph nodes suggests that cancer may have spread through the lymphatic system to other parts of the body. However, it's important to understand that not all women with cancer cells in their lymph nodes will experience metastasis, and conversely, some women without cancer cells in their lymph nodes might develop metastases. The behavior of breast cancer is influenced by various factors, including the type of cancer, its stage, the aggressiveness of the cells, and the overall health of the individual. The majority of breast malignancies fall under the category of carcinomas, which are cancers that originate in the epithelial cells lining the organs and tissues. Carcinomas account for a significant proportion of breast cancers [14–15]. These cancers can be further classified into different subtypes based on their specific characteristics, which aids in tailoring treatment approaches to individual patients. In conclusion, breast cancer is a complex and heterogeneous disease that arises from abnormal cellular growth within the breast tissue. It can spread through the lymphatic system, which plays a key role in draining fluids and

maintaining immune function. The presence of cancer cells in lymph nodes is an important indicator for assessing the potential for metastasis, but individual outcomes can vary widely based on multiple factors. The majority of breast cancers belong to the carcinoma category, reflecting their origin in epithelial cells.

2.2.4 Chemotherapy

Chemotherapy is a form of treatment that uses anti-cancer medications to kill cancer cells [16]. Anti-cancer medications used in chemotherapy may be either orally or intravenously. Most cancer cells in the body are reached by the medications through the blood stream. Chemotherapy may be injected directly into the spinal fluid, which surrounds and protects the brain and spinal cord in the event that cancer has spread there. Not all breast cancer patients will require chemotherapy. There are several conditions for which chemotherapy may be suggested [17]. After surgery (adjuvant chemotherapy), which might be given to try to eliminate any cancer cells that might have been left behind or have spread but cannot be seen, These cells may develop into new tumors in other parts of the body if they were allowed to flourish. Breast cancer recurrence can be reduced with adjuvant chemotherapy. Chemotherapy (neo adjuvant chemo) may be recommended prior to surgery. This might be given to try to shrink the tumor so it can be removed with less extensive surgery. As a result, neo adjuvant chemotherapy is usually used to treat malignancies that are too large to be surgically removed, when first diagnosed, have a large number of cancerous lymph nodes, or have other inflammatory breast cancers [17].

2.2.5 Cell membrane

Every cell has a membrane around it that both identifies it spatially and delineates the boundaries between intracellular and extracellular space. Lipids and proteins make up these membranes [18]. It is crucial for cellular defense, nutrition regulation, and transport. Cell membranes are engaged in a number of processes, such as membrane fusion, enzyme catalysis, molecular recognition, and cellular adhesion. Cell membranes exhibit extremely complicated composition in terms of lipids and proteins. The hydrophilic head group and the hydrophobic region make up the amphiphilic nature of membrane lipids. Membrane lipids self-assemble into a bilayer in aqueous medium due to their amphiphilic nature and their geometric limitations [19]. The membrane lipids are organized into a continuous bi-layer (Fig. 1.1), phospholipids that have hydrophilic sections that are submerged in water and hydrophobic regions that are protected from the aqueous environment.

There are two types of proteins that are introduced into this lipid bilayer: integral proteins and peripheral proteins

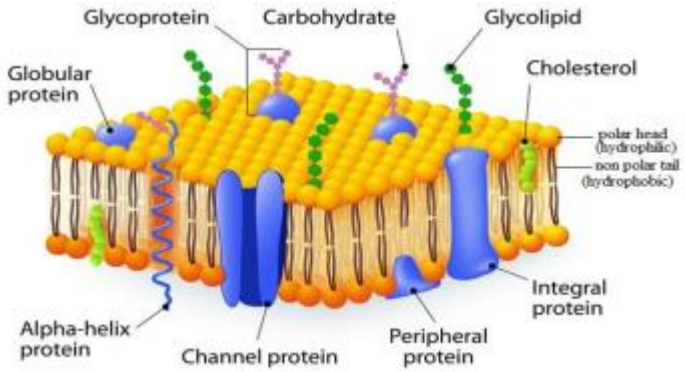

Figure 1.1Mosaic model of membrane structure and lipid bilayer [20]

Integral proteins become associated with membranes through a direct interaction with the lipid bilayer. Some of these proteins span the complete thickness of the membrane, often traversing it multiple times [20]. Alternatively, others are situated closer to the membrane's exterior or interior. These integral proteins possess amphipathic characteristics, featuring two hydrophilic ends separated by a hydrophobic region that crosses the hydrophobic core of the bilayer. The hydrophilic ends of the integral protein are positioned outside the membrane on either the internal or external surface. Integral proteins fulfill the role of channels, permitting specific ions to traverse the membrane [20]. In the lipid bilayer, phospholipids do not engage in direct interactions with peripheral proteins. Instead, they establish connections with integral proteins through electrostatic contacts. These peripheral proteins can be found on both surfaces of the membrane. Peripheral proteins play a pivotal function in cell adhesion, anchoring cells to each other and to the basal lamina. These proteins, which serve as cell adhesion molecules [20], contribute to the anchorage of cells and the maintenance of the structural integrity of cellular arrangements.

2.2.6 Membrane potential

One of the fundamental characteristics of living cells is the membrane potential, or the difference in potential between the external and intracellular compartments. The underlying mechanisms (pumps, ions channels), whereas practically all cells have a negative membrane potential, differ depending on the kind of cell. [21]. Because of a network of ion pumps and channels, the plasma membrane of the cell experiences resting transmembrane voltage (electric potential difference) when it is not exposed to an external electric field [20]. An imbalance in the electric charge between the intracellular and extracellular media occurs when a cell is at rest as a result of the interaction of diffusion and electric force. As a result, the membrane creates a potential difference known as membrane potential.

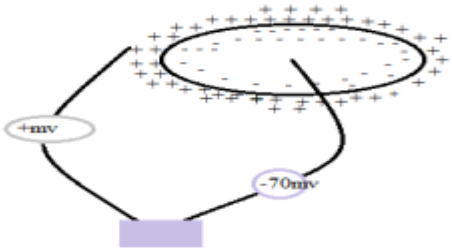

Figure 1.2 Rest potential: intra- and extracellular potential of a cell in normal conditions [20].

The majority of biological cells tend to maintain a resting potential that falls within the range of -35 mV to -90 mV [20]. This resting potential reflects the intracellular medium's negative charge, and this negativity arises from the prevalence of activated chloride (negative) ion pumps compared to sodium or calcium (positive) ion pumps at rest [20]. When the membrane potential of a cell becomes more positive (less negative), it's referred to as depolarization, whereas when the membrane potential becomes more negative (less positive), it's called hyperpolarization [20]. Changes in ion concentrations and alterations in the surface charge of the cell membrane can modify the resting potential value through depolarization, which involves the activation of voltage-gated ion channels [20]. The activation of these voltage-gated ion channels leads to changes in membrane polarization and the closure of these channels, which is influenced by shifts in intracellular ion concentrations [20]. Action potentials occur as ions briefly move along their concentration gradients, giving rise to variations in signaling and transduction pathways [20]. Particularly, the concentration of calcium ions (Ca2+) plays a crucial role. Fluctuations in

intracellular Ca2+ concentrations bring about changes in various cellular processes, including migration, proliferation, cell attachment, necrosis, and apoptosis [20].

2.2.7 Electrical properties of cancer cells

Normal cells have the ability to communicate both internally and externally, as well as with other cells. The coordination of information among the body's cells plays a crucial role in regulating and integrating cellular functions, including cell growth. However, when cancer develops, the usual control mechanisms no longer apply to cancer cells. In fact, cancerous and rapidly proliferating cells have lower cell membrane potentials compared to normal adult cells. Cancer cells also exhibit distinct characteristics that set them apart from typical rapidly dividing cells. While normal cell proliferation is well-organized, cancer cells are more loosely connected and do not maintain contact as they grow. They no longer adhere to the signaling and growth control mechanisms found in healthy tissues, essentially losing coordination with the rest of the body [22]. One noticeable difference lies in the electrical properties of cancer cells, which are distinct from those of surrounding healthy tissues. Cancer cells tend to have higher intracellular sodium levels, a greater presence of unstructured water, lower concentrations of intracellular potassium, magnesium, and calcium, and more negatively charged cell surfaces. Furthermore, cancer cells exhibit abnormal transmembrane potentials and membrane permeability, both of which are lower than those of normal cells. In contrast, healthy cells possess higher membrane potentials than cancer cells, resulting in a reduced electric field within the membrane of cancer cells [22]. It's worth noting that the concept of categorizing cancers based on their electrical characteristics is not a new one. In fact, this idea was initially proposed in 1926 by Fricke and Morse. Studies have shown that malignant tissue possesses higher electrical conductivity and permittivity compared to normal tissue. Due to their greater permittivity, which refers to their ability to resist the development of an electrical field, cancerous cells exhibit distinct resonation patterns from healthy cells [22].

2.2.8 Electromagnetic interaction an electrical property of cells

Maxwell's equations were used to predict how electromagnetic waves would move as they carried energy. An electromagnetic wave with total energy density, u, can transfer energy to objects in its path. The electromagnetic wave is

$$u = \frac{1 \in E^2}{2} + \frac{B}{2\mu^2} \qquad 1$$

Electromagnetic waves display varying characteristics based on their wavelength or frequency. When these waves interact with a medium containing ions and electrons, the Lorentz force comes into play. In dielectrics, electrons are bound to nuclei, restricting their movement. Yet, even these electrons respond to external fields, inducing a small current. Light's journey through tissues is influenced by scattering, reflection, absorption, and fluorescence. At the interface of materials, a discontinuity in refraction causes a portion of incoming light to reflect while the rest transmits. The extent of surface-reflected incident power relies on factors like polarization, angle of light

incidence, refractive index of the medium and material [23]. Laser energy mostly penetrates biological tissues, and this penetration is guided by tissue optical properties: light absorption, scattering anisotropy, and refractive index. Laser-tissue interactions are classified by wavelength, a crucial determinant due to molecular absorption. Molecules such as DNA and proteins, prevalent in tissues, absorb strongly around 200 nm. Oxygen consumption is stimulated at 365 nm, possibly involving mitochondria. The absorption peaks of biomolecules and tissues are wavelength-driven. Most biological tissues exhibit optical scattering from 400 to 1100 nm [24]. Near-infrared radiation (NIR), ranging from 750 to 2500 nm, impacts mammalian cells with low-energy radiation. NIR fosters keratinocyte proliferation, enhances cell attachment, and aids cardiac infarction recovery in animals. Skeletal muscle regeneration and proliferation are also triggered. NIR displays effects on advanced neoplasia. Research uses a 915 nm laser to explore NIR's influence on pancreatic cancer cells. This laser induces caspase-3 activation and apoptosis. Combined with gemcitabine treatment, the 915 nm laser increases apoptotic cell count. The study proposes a promising avenue for cancer therapy, employing infrared and chemotherapy together [25].

2.2.9 Electro portion

In a process known as electro portion or electro permeabilization, the cell membrane becomes more permeable to ions and large molecules when exposed to a brief, high-voltage electric field impulse. Initially, the creation of hydrophilic in the lipid bi layer causes an increase in permeability. When a cell exposed to an external electric filed leads to an induce voltage across the cell membrane which is super imposed on the resting transmembrane voltage [26]. Agues pores are brought on by the rearmament of the cell membrane, which lead to very important increases the membrane permeability. Poration improves the membrane's conductivity and permeability to water-soluble molecules, without which the membrane transport mechanism would not function [27]. When the transmembrane voltage hits a critical level, electroporation can occur in the membrane, causing the inter dielectric to break down in a matter of seconds and increasing the membrane conductivity. [28].With membranes, the irreversible rupture of the membrane caused by voltages is also observed [29].

2.3 Laser trapping Techniques

Through its emission, scattering, and absorption, light can act as a force on matter; After Ashkin's 1986 development of the laser, this force was experimentally demonstrated. Experiments have been widely used to examine the interaction of light and matter, leading to the invitation of accidental procedures that have had a significant impact in a variety of domain [30]. Since roughly 20 years ago, micron and submicron atoms have been manipulated and studied using the optical trapping of microscopic particles by the pressure of laser radiation. Biological particles in aviaries and micron sizes can also be captured and controlled by a single-beam gradient trap [31]. Optical traps are used to manipulate microscopically sized objects without physical contact. In biology, an optical trap provides a new and innovative tool for manipulating organisms and cells. Ashkin et al. claimed that Ashkin was the first to define the optical trapping of micrometer-sized particles utilizing the radiation pressure from the two competing laser beams. While the single-beam gradient force trap atom was also proposed [32]. Optical force has been used to study the structural characteristics of biological polymers such as DNA, molecular motor membranes, and whole cells. The micro rheological characteristics of these objects can be investigated up through the application of force either to the object itself or to a small dielectric sphere or bead to which the object is attached [33]. The gradient force is alluring when the particles refractive index higher than that of the surrounding medium. The gradient force pulls on the dielectric particle at the center of the trap, whose strength is proportional to the applied electric field. The gradient force pushes the particle if its refractive index is lower than that of the medium. When the particle is extremely small in comparison to the light's wavelength, the Releigh regime is employed ($R << \lambda$). The limiting regime of particles significantly larger than the wavelength of ($R >> \lambda$) can only be described by the ray optics regime. The optical rays have a changing direction after the encounter, and some of their photon momentum (h/λ) is transmitted to the object. The net optical force contracts the displacement of the bead from its equilibrium location in the center of the trapping beam as it is steered towards a focused Gaussian beam [33].

2.3.1 NIR Laser irradiation of cancer cells and chemo therapy

Middle Tennessee State University conducts research on the non-toxic substance 2-dodecyl-6-methoxycylohexa-2, 5-diene-1, 4-dione (DMDD), which can slow the growth of human breast cancer cells. The toxicity and efficacy of DMDD in treating metastatic breast tumors were investigated using an in vivo animal model of the 4T1 mammary carcinoma. DMDD significantly extended the lifespan of 4T1 tumor-bearing mice without causing any obvious damage. DMDD significantly inhibited the growth of 4T1 cells in vitro while reducing breast tumor growth and metastasis in animals. The serum levels of (TNF-, IL-6, IL-12, TGF-, and VEGF) were regulated by DMDD. The immune response to chemical testing revealed a relationship between the activation of Bax, calved caspases-3 and-9, dawn modulation of Bcl-2, MMP-2 and 9, NF-kB, and the deactivation of NF-kB pathways and the suppression of tumor growth and metastasis. As a result, the expression of numerous genes that inhibit apoptosis and promote metastasis, including Bcl-2 and MMPs, demonstrated that DMDD may be an effective and safe anti-tumor drug when used to treat late-stage breast cancer [34]. In the in vitro study, five types of cultivated cancer cell lines (MCF7 breast cancer, Hela uterine cervical cancer, NUGC-4 gastric cancer, B16FO melanoma, and MDA-MB435 melanoma) were irradiated using the infrared device, and then the cell proliferation activity was evaluated by the 3-(4,5 dimethylthiazol-2yl)-5-(3-corboxymeth-axyphenyl)-2-(4-suitophenyl)-2h-tetrazolium (MTS) assay. The proliferation rate of all cancer cell lines was significantly decreased by infrared radiation [35]. A very promising use of near-infrared laser-induced photo thermal therapy (PTT) is the ablation of solid malignancies. However, tumor recurrence and unsatisfactory outcomes are the result because light thermal therapy is unsuccessful at destroying all tumor cells due to the non-uniform heat distribution over tumors. To improve the effectiveness of tumor treatment, photo thermal therapy (PTT) should be developed in conjunction with other modalities. Especially when taking medications for chemotherapy. A paper claims that smart DOX/IR-780-loaded temperature-sensitive liposomes (DITSL), which can achieve NIR-laser-controlled medications, can be used for chemo photo thermal synergistic tumor therapy. The core of this system contained the hydrophilic component: the water-soluble chemotherapeutic agent doxorubicin (DOX), whereas the lipid-soluble IR-780 was incorporated into the temperature-sensitive lipid layer. The resultant DITSL exhibited stability within physiological conditions and could efficiently release substantial amounts of DOX in a controlled manner, both in PBS and cellular environments. This study underscores the potential of nanoparticles as a means

to treat tumors, as evidenced by the significant reduction in tumor growth in vitro and in vivo when using temperature-sensitive liposomes loaded with DOX (DTSL) or IR-780 (ITSL) [36]. B16F10 cells were subjected to continuous laser radiation in a controlled environment over three consecutive days. The cells were placed in 12-well plates for trypan blue and cytometric assays and 96-well culture plates for the MTT technique. The laser operated with a constant wave output of 50 mW, with a beam spot size of 2 mm2, and an irradiance of 2.5 W/cm2. An aluminum sheet was placed halfway between the wells, which were separated by 5 cm in all directions. The control group of wells was randomly exposed to a low-level laser therapy (LLLT) dose of 150 J/cm2, with an irradiance of 2.5 W/cm2 for 60 seconds. Meanwhile, the second group received LLLT doses of 1050 J/cm2 and 2.5 W/cm2 for 420 seconds. Across the irradiated groups, the total energy delivered after all three sessions amounted to 9 J and 63 J, respectively. Interestingly, there were no statistically significant differences in the total count of B16F10 cells observed using either the trypan exclusion method or the MTT colorimetric assay when comparing the irradiation groups and control groups at various time points. In terms of cell cycle analysis within B16F10 cells, no significant differences were found between the irradiation groups and the control group at 24 h, 48 h, and 72 h. However, after 72 hours, a statistically significant distinction emerged between the irradiation group and the control groups (8.48±1.4% and 4.2±0.6%) in terms of the proportion of hypo diploid cells, indicative of possible cell death. Notably, the increase in apoptosis was most pronounced at the lower energy level of 150 J/cm2 [37].

CHAPTER THRE

3.1MATERIALS **AND METHODOLOGY**

In this chapter, I'll discuss an experiment that involves treating pre-ionized breast cancer cells within 24 hours. I'll also discuss the materials used in the experiment and the mechanism by which the membranes break down.

3.2 4T1 breast cancer cell cultivated and treatment

The sample was cultivated and treated at the Tennessee center for Botanical medicine researches international ginseng institute, and the laser trapping experiment was carried out in the department of physics and astronomy, middle Tennessee state university. The cells were incubated in the humidity atmosphere with 5% CO_2 and 37^0c, 4T1 cancer cells where grown in RPMI 160 media, supplemented with 10%fetal bovine serum (FBS). Trypsinization, or the act of dissociation cells using trypsin was performed on the cells in the container (vessel) in which they are being cultivated. Every 2-3 days the passaged (a sub culture is a new culture created by transferring part or all of the cells from an earlier culture to fresh growth medium). 4T1 cells were diluted with RMPI 160 medium after being trypsinized. And seeded in a 96- well plate with in an intensity of 5000-7000cells per well (100µL/well). Cells were treated with DMDD at100µ moles for 24. After the cells were anchored to the bottom of the wells for 24h hours. The 24 h treatment of 4T1 cells had six replicate wells. Following the treatment, cultured medium. The wells were transferred to Eppendorf tube. Next, the wells were rinsed with phosphate buffered saline (PBS) and 50µL trypsin was added to each well, the detached cells were transferred to the same Eppendorf tube.

3.3 Experimental set up and materials

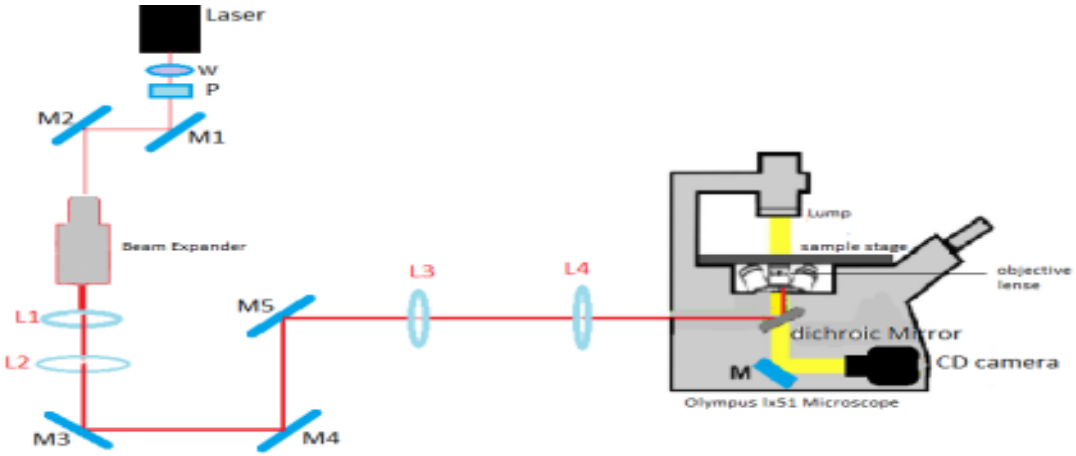

Figure3.1 Aschematic of laser trap experimental set –up

Figure 3.1 illustrates the arrangement of the laser trap setup. We utilized a diode-pumped infrared laser operating at a wavelength of 1064 nanometers (Spectra Physics V-extreme Nd: YVO4 laser).This laser generates a linearly polarized beam with a width of 4 mm and a maximum power output of 8 W. Control over the beam's power was achieved using a polarizer (P). To expand the beam, a 20X beam expander along with a pair of lenses (L1 and L2) having focal lengths of 5 cm and 20 cm, respectively, enlarged the beam size to approximately match the diameter of the microscope's objective lens window (2 cm). This step was crucial to establish a stronger trapping effect. To improve beam alignment, mirrors M3 and M4 were employed for refocusing, and M5 was strategically positioned to enable the creation of a controllable trap at the microscope's focal plane. M5 was situated 20 cm away from the third converging lens (L3), which was placed at a distance from another converging lens (L4) with a focal length of 20 cm. The separation between L3 and L4 equaled twice their respective focal lengths, a configuration designed to establish a steerable trap precisely at the microscope's focus plane. To link the collimated and aligned beam to the microscope, a dichroic mirror (DM) was employed at a 45-degree angle within the microscope. This mirror served to reflect the laser beam at a normal angle of incidence to a 100X objective lens with a numerical aperture of 1.25. The DM also transmitted imaging light from an Olympus Tl4 halogen lamp through the second port of the microscope, enabling real-time imaging captured by a PC-controlled digital camera integrated into the microscope. For experiments involving cell trapping and ionization, power measurements were taken at two distinct locations.

The first measurement was conducted before the beam reached lens L4 (4.34 W), while the second measurement was obtained after the beam exited the objective lens (0.806 W).

3.4 How the optical trap works

It can be works in two ways

In Figure A, we observe a fundamental ray optics diagram. Two rays labeled as 'a' and 'b' converge at position 'f' due to the focusing action of the objective lens, when there's no bead present. This position 'f' represents the actual laser focus point. However, when the rays pass through the bead, they experience refraction, causing the new focus to shift to the right of position 'f'. After interacting with the bead, ray 'a' is bent upwards and towards the right of its original trajectory, while ray 'b' is deflected downwards and to the right. The forces exerted on the bead by rays 'a' and 'b' are denoted as 'Fa' and 'Fb', respectively. The combined force, represented by 'F total', is the vector sum of these two forces and points to the left.

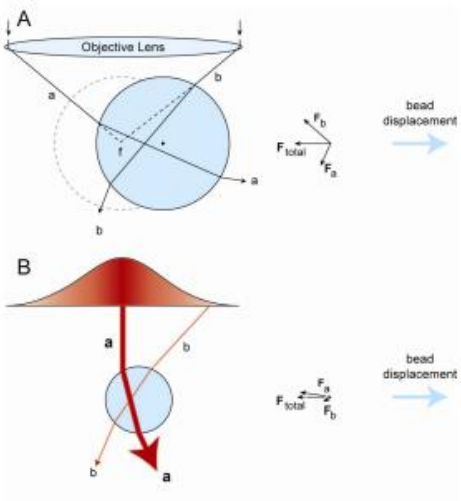

Figure 3. 2the simplified illustrations of optical trapping [38]

Moving on to Figure B, we examine the force within a single-beam gradient optical trap that features a Gaussian intensity profile. Here, two rays are depicted. The central ray, denoted as 'a', experiences a higher intensity compared to the outer ray, labeled as 'b'. As a result, the bead is once again displaced to the right of the true laser focus. Despite this displacement, the total force acting on the bead, represented by 'F total', continues to point towards the left [38].

2. The rays a and b are refracted such that the new focus with in the bead lies below f. and more convergent up existing the bead. This slight refocusing of the laser causes a force on the particle

pointing up wards, towards the laser focus f. the opposite is true when the particle is above the focus and the ray becomes more divergent in figure 3.2

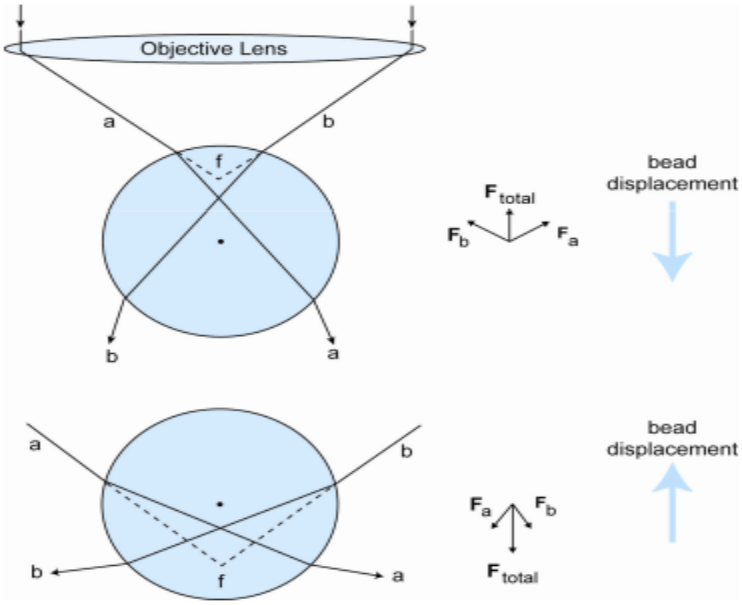

Figure3. 3 *description of axial trapping force [38]*

The degree of divergence of the focused laser light undergoes changes based on the axial movement of the bead within the optical trap. In the absence of the bead, the two rays labeled as 'a' and 'b' are focused by the objective lens onto position 'f', which corresponds to the true laser focus.

In Figure 3.3A, the bead introduces refraction causing the new focus to be positioned below the initial laser focus. When the bead is present, the two rays converge more, resulting in ray 'a' being bent downwards and towards the left, while ray 'b' is deflected downwards and to the right. The forces 'Fa' and 'Fb' represent the influences on the bead by rays 'a' and 'b' respectively. The combined force, 'F total', is the sum of these two vectors and points upward.

Moving to Figure 3.3B, when the bead is positioned above the laser focus, the deflected rays 'a' and 'b' diverge further. As a result, the net force points downward. As the light passes through the particle, it undergoes refraction and some of it is reflected backwards. This scattering force, associated with these reflected rays, pushes the particle away from the laser focus. Consequently, the center of the optical trap is established at an axially displaced position from the original focus point [38-39].

3.5 Mechanisms of membrane break down

Membranes are made by nature to be stable and resist external constraints. They must be destabilized, which means they must be made to modify their structure. We have various methods for destabilizing membranes. One of them is polarization.

3.5.1 Polarization due to restricted motion of charges.

External electric field can induce formation of pores in membranes, move cells by electrophoresis. Electric fields and charges fundamentally interact with one another to cause membrane polarization. Electric field exert force on charges which can either move if they are free or accumulate if they are limited in their motion. Charge redistribution in constrained space is characterized by its polarizability, whereas the free transport of charges depends on the conductivity of the material.

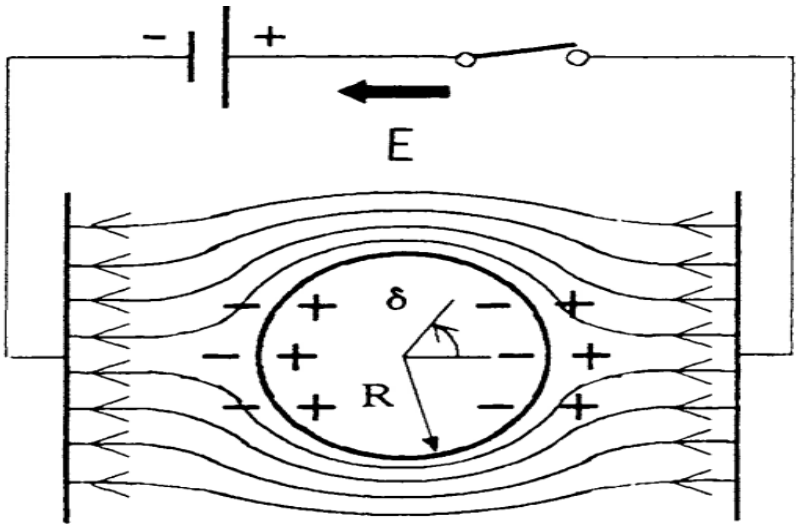

Figure3. 4 shows membranes restrict motion of charges and lead to cell polarization by external electric fields [40]

3.5.2 The interaction of electric fields with polarized membrane

Forces are produced when external electric fields interact with polarized materials, which can induce motions in side particles or motion of the particles as a whole. The movement within the material may cause mechanical fracture or structural rearmaments in the substance, which for membranes can subsequently lead to their electro poration and electro fusion. The motion of the particle as a whole can occur in the absence of a net charge but only non-uniform electric fields. It is a consequence of the interaction of re distributed charges, which have zero net charge but locally interact with electric fields of different strengths, which leads to net force exerted on the particle. This phenomenon is named di electrophoresis, can also occur in homogenous external fields. If there are other particles yielding local non-uniformities of the electric field, this leads the mutual attraction of the particles to their approach and eventually to adhesion.

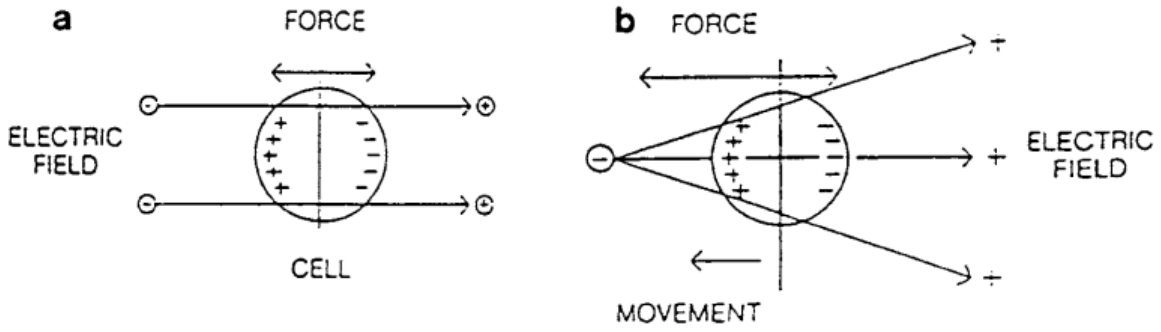

Figure3. 5 shows charge separation and force on a cell in (a) homogenous (b) an in homogenous electric field [40]

The electric field determines the size and type of motion. It is also depends on the nature and the geometry of material. Membranes are surrounded by a medium with a high dielectric constant (80), a low conductivity (specific membrane conductance of roughly 1mS/cm^2), and low polarizability (relative dielectric constant of 2) [40]. The breast cancer cell membranes damaged by the drug to some level. This is essential to lowering the radiation energy that breaks dawns the membrane. Following the treatment, the cell was irradiated with a high power laser using a trapping techniques. The membrane is break down by the powerful electric field at the focus point [41].

CHAPTER FOUR

4.1 RESULT AND DISCUSSION

In Section 3.1, a sample culture of 4T1 breast cancer cells was discussed. The digital camera took sequential images of the 24 hr-treated breast cancer cells at a fixed grabbing rate of 8 frames when the cells entered the laser trap. Real-time images of the 24-hour-treated breast cancer cells illustrating these processes are shown in Figure 4.1 for the 24-hour-treated breast cancer cells

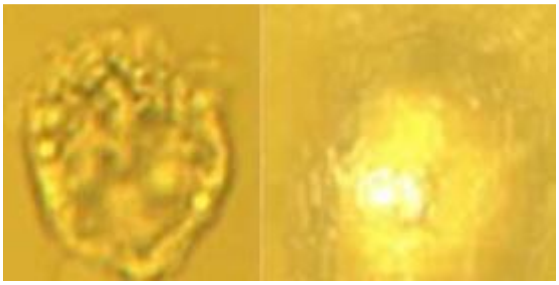

Figure 4.1shows the images apprehended for 4T1 breast cancer cells before and after trapping, respectively

From figure 4.1, we observed that the area of the cell after trapping is smaller than the area of the cell before trapping. Our objectives were to study the electrical property of 24-hour-treated breast cancer cells before they ionized using the laser trapping techniques and to form the equation of motions of cells.

We analyze 27 4T1, 24-hour-treated breast cancer cells, and their shapes are considered to be spherical. The area of the cells before and after trapped were measured using image of pro plus 6 in pixels. The radius was found from the area of the cells. The cells were tracked as they are moving to the trap. Using origin 2019b, the velocity, and the acceleration of each cell was calculated from the measured displacement. We calculate the relationship between meter and pixel from the snap shoot image size and the real size of 3.1-mm silicon beads and we have got 7.27×10^{-8} meter/pixel. This conversion factor used to convert pixel to meter. The mass of each cell is found out by

$$M_{cell}=\rho V_{cell} \qquad 4.1$$

Where the density of the cancer cells $\rho=1081 kg/m^3$

Table 4.1 shows that the data of the area before and after trapping, mass and volume of 24-hourly treated breast cancer cells.

	24 hour treated breast cancer cells (27)				
Quantities	Mean	Standard deviation	Min	Median	Max
Area before (μ m^2)	166.114	60.2813	76.779	153.025	316.211
Area after (μm^2)	84.4993	46.673	21.5191	70.1529	186.565
Mass(nkg)	0.366288	0.343319	0.106878	0.201463	1.53972
Volume(μm^3)	1685.46	930.506	506.20	1424.35	4230. 96

Table 4.1the statically data of the area before and after trapping, mass and volume of 24 hourly treated breast cancer cells.

4.2 The dynamics of pre-ionized, 24 hourly treated breast cancer cells

The cell inters to the trap in the direction of the laser electric field. This applied electric field induces polarization charge as a result the induced electric field generates. The strength of induced electric field increase as the cell approaches to the trap and also the oscillation of the dipole moment increase. The direction of induced electric field is opposite to the applied one. The velocity of the cells decreases due to two reasons, the first one is due to induced electric field which decrease the trapping force. The second reason is around the trap the strong electric field start to breakdown the dipole oscillations that build the free charge on the cells and the Coulomb force oppose the trapping force hence the cells decelerate near the trap. Membrane breakdown is helped by DMDD (2-Dodecyl-6-methaxycyclohexa-2, 5-diene-1, 4-Dione) treatment. The charge ensuing from such membrane breakdown in 24-hour-treated breast cancer cells is the summation of the polarization charge and free charge. In this section, we wish to study the magnitudes of the charge developed and spring constant of each cell (coefficient of the trap) by analyzing the pre-ionization dynamics of each cell. The pre-ionization dynamic quantities such as displacement, velocity, and acceleration depend on the charge and spring constant. Using different methods, we have studied the quantities to determine the charge developed in each cell and the spring constant (coefficient of laser trap). The methods are as follows: first, we solve the equation of motion r(t) of the 24 hr treated breast cancer cell, and then, using a nonlinear curve fitting model, we fit the displacement verses time data for the equation of motion r(t).Finally the charge and spring constants (coefficient

of laser trap) are determined. The second method is that, using Origin Pro 2019b from the first and second derivations of the displacement vs. time data, the velocity and acceleration of each cell are determined.

4.2.1 Results and discussion

Figure 4.2 displays an example of pre-ionized breast cancer cell sequential images that illustrate a cell's travel, where the trapping point of the sequential snapshots is connected by a horizontal red line. The cell is entering the laser trap; its trajectory follows the polarization direction of the trapping laser for a flawlessly aligned trap, which is indicated by the green line. The trap, drag, and the electrical force acting on the breast cancer cells define this trajectory. For the pre-ionization dynamics, we are interested in two electrical properties of 24-hour-treated breast cancer cells. This is the net charge developed on the cell and the spring constant (coefficient of trap) due to the dielectric breakdown ensuing from the pre-ionization of 24-hour- treated breast cancer cells.

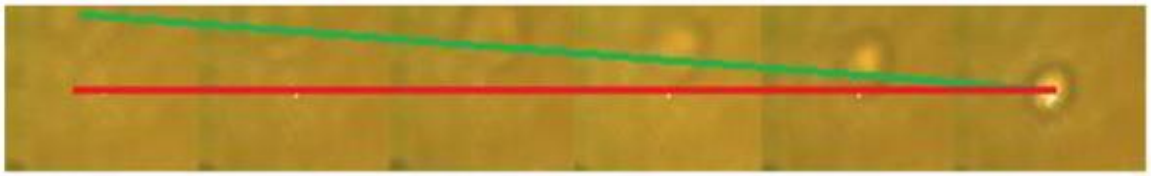

Figure 4.2 the motion of the cells when they are moving into the laser trap

To determine both the charge and the spring constant of each breast cancer cell. We measure the displacement as a function of time when the cells are moving to the trap. The average measured values of radius, area, volume and mass of the breast cancer cells are 7.16μm, 166.114 μm^2, 1685.46 μm^3 *and* 0.366288 nkg respectively.

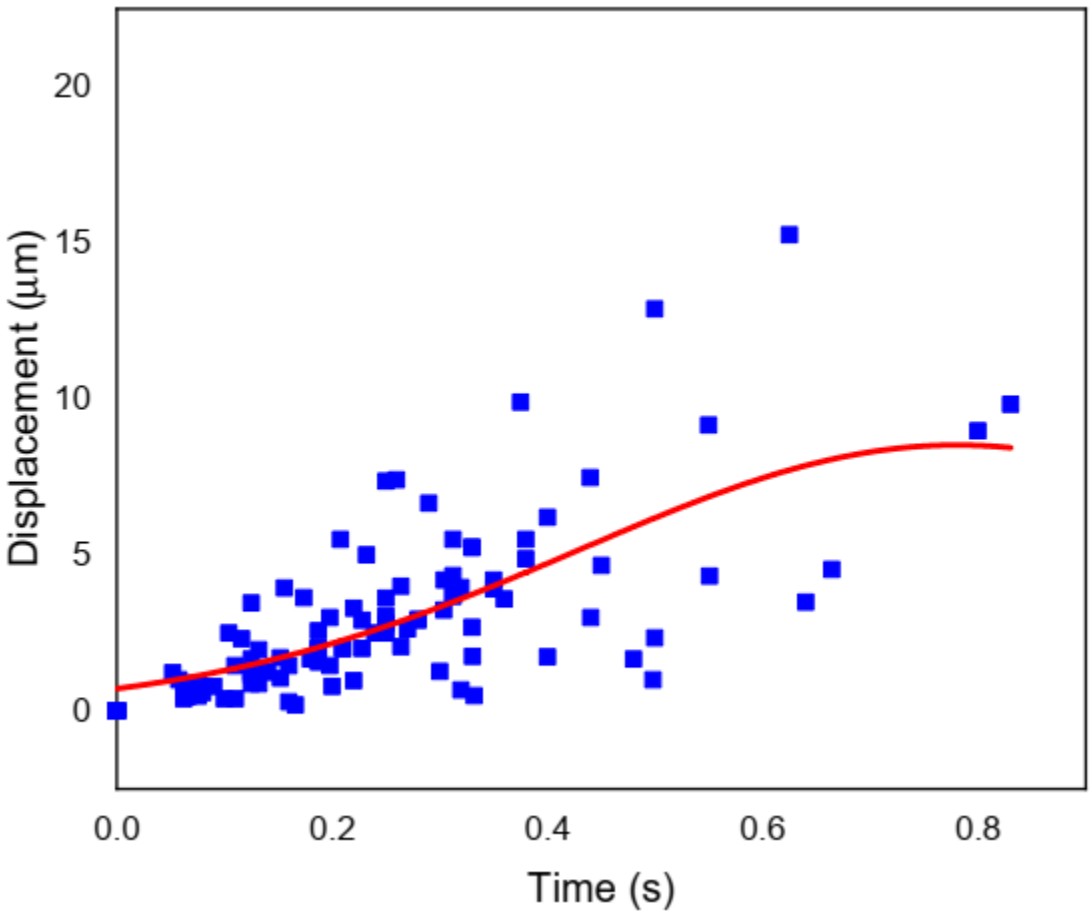

Figure 4.3displacement for all 24-hr treated 4T1cancer cells as measured from the pre-ionized to the center of the laser trap as a function of time

Figure 4.3 shows that the displacement time graph for all the breast cancer cells when they are moving into the laser trap. As shown in the graph, the cells accelerate for the first some points and then immediately starts to decelerate until it trapped. Each cell has its own level of membrane breakdown and polarization as the result the magnitude of displacement of each cell differ. Based on the change displacement with time and the size of the cells, we determine the trapping and electrostatic forces. The average measured radius of breast cancer cells is 7.16µm, and the average velocity is 15 µm/s. The beam radius (w) determined at the site of the trap using this average cell size is 243.2µ m. .

$$F(r) = kr \qquad 4.2$$

Equation 4.2 is the trapping force that continuously tries to pull the cells into the center of the trap. The trapping force is mainly depending on the electric field strength that decreases away from the center of the trap. When cells move toward the center of the laser trap, the constant k is the trapping

force coefficient that depends on the size of the induced polarization. It can also be determined by the dielectric susceptibility of a pre-ionized cell and the size of the electric field in the trap. The constant k differs from one cell to another. It also has greater induced electrical polarization as it moves towards the center of the trap. This induced polarization is mainly due to the electric field of the laser trap. Which could be decreased or increased by the net charge developed on each cell. Like constant k, the charge developed on each 24 hr treated breast cancer cell differs from one cell to another depending on the area of the cells and on the extent of membrane break down in the cells.

Electrostatic **force;** when the cell is moving toward the trap, it be ionized by electromagnetic field radiation. Because of membrane breakdown, there is a charge buildup.

$$\vec{F}_e(r) = qE_0 \tag{4.3}$$

The amplitude of electric field at the trap location can be stated as

$$E_0 = \sqrt{\frac{2pv\mu o}{A}} \tag{4.4}$$

Where v is the speed of light in the medium that the cells are suspended in, and A is laser beam area, μ_o is the magnetic permeability of free space and p is the power of the trap.

Drag force, the shapes of the pre ionized breast cancer cells are being spherical with the radius R and the drag force can be indomitable using

$$\vec{F}_d = 6\pi\mu R\frac{d\vec{r}}{dt} \tag{4.5}$$

Where μis the viscosity of the fluid that the cell is suspended in to be on the same order of water, which at room temperature is $1x10^{-3}NS/m^2$

$$\beta = 6\pi\mu R \tag{4.6}$$

The force, the cells are at rest and trapped by the laser gradient force**.** It becomes ionized, and the electrostatic force increases due to the development of more charges on the cells. At the same time, it also experiences a drag force. Thus the pre-ionized dynamics can be summarized according to Newton's second law, the net force that is performing on the 24 hr treated breast cancer cells before it is ionized using the equations of (4.2), (4.3), and (4.5) can be written as

$$\vec{F} = \vec{F}_t - \vec{F}_d - \vec{F}_e \tag{4.7}$$

$\vec{F}$ is net force acting on the cell. The trapping force pulls the cell to the trap, the drag and electrostatic force due to the free and polarization charge on the cell.

$$m\frac{d^2\vec{r}(t)}{dt^2} = kr(t) - \frac{\beta d\vec{r}(t)}{dt} - qE0 \quad 4.8$$

$$m\frac{d^2\vec{r}(t)}{dt^2} + \beta\frac{d\vec{r}(t)}{dt} - kr(t) = -qEo \quad 4.9$$

Where r is the displacement from the pre-ionized, 24-hour-treated breast cancer cells to the center of the laser trap, β is the coefficient of the drag force, m is the mass of the pre-ionized, 24-hour-treated breast cancer cells and k is the spring constant (coefficient of trap) of 24-hourly-treated breast cancer cells.

$$\frac{d^2\vec{r}(t)}{dt^2} + \frac{\beta d\vec{r}(t)}{mdt} - \frac{kr(t)}{m} = -\frac{qEo}{m} \quad 4.10$$

This is in homogenous second order differential equation, thus to find the general solution of we should find its complementary and particular solutions. Therefore, the complementary and particular solutions are

$$r_c(t) = e^{\frac{-\beta t}{2m}}\left[\left(Ae^{\frac{\sqrt{\beta^2+4km}}{2m}t}\right) + \left(Be^{-\sqrt{\frac{\beta^2+4km}{2m}}t}\right)\right] \quad 4.11$$

$$r_p(t) = \frac{qEo}{k} \quad 4.12$$

The general solution of equation 4.10was found by adding equations 4.11 and 4.12

$$r(t) = e^{\frac{-\beta t}{2m}}\left[\left(Ae^{\left(\frac{\sqrt{\beta^2+4km}}{2m}\right)t} + Be^{-\left(\frac{\sqrt{\beta^2+4km}}{2m}\right)t}\right)\right] + \frac{qEo}{k} \quad 4.13$$

To fix the value of the coefficients A and B, we assume that the initial displacement and velocity of the pre-ionized, 24 hour treated breast cancer cells at a time (t) = 0 are both zero. So the value of coefficients of B and A are

$$B = \frac{qE0}{2k}\left[\frac{\beta}{\sqrt{\beta^2+4km}} - 1\right] \quad 4.14$$

$$A = -\frac{qEO}{2k} - \frac{qEO}{2k}\left(\frac{\beta}{\sqrt{\beta^2+4km}}\right) \quad 4.15$$

By substituting equ.4.14 and equ.4.15in to equ.4.13 we can obtain the equation motion of the cells before they trapped.

$$r(t) = \frac{qEO}{k}\left\{1 - e^{\frac{-\beta t}{2m}}\left[\frac{1}{2}e^{\sqrt{\frac{\beta^2+4km}{2m}}t} + \frac{\beta}{2\sqrt{\beta^2+4km}}e^{\sqrt{\frac{\beta^2+4km}{2m}}t} + \frac{1}{2}e^{-\sqrt{\frac{\beta^2+4km}{2m}}t} - \frac{1}{2}\frac{\beta}{\sqrt{\beta^2+4km}}e^{-\sqrt{\frac{\beta^2+4km}{2m}}t}\right]\right\} \quad 4.16$$

$$r(t) = \frac{qEO}{k}\left\{1 - e^{\frac{-\beta t}{2m}}\left[\frac{e^{\sqrt{\frac{\beta^2+4km}{2m}}t} + e^{-\sqrt{\frac{\beta^2+4km}{2m}}t}}{2} + \frac{\beta}{\sqrt{\beta^2+4km}}\left(\frac{e^{\sqrt{\frac{\beta^2+4hm}{2m}}t} - e^{-\sqrt{\frac{\beta^{2+4km}}{2m}}t}}{2}\right)\right]\right\} \quad 4.17$$

We can write the exponential term $\frac{e^{\sqrt{\frac{\beta^2+4km}{2m}}t} + e^{-\sqrt{\frac{\beta^2+4km}{2m}}t}}{2} = \cos h\sqrt{\frac{\beta^2+4km}{2m}}t$ and $\frac{e^{\sqrt{\frac{\beta^2+4hm}{2m}}t} - e^{-\sqrt{\frac{\beta^{2+4km}}{2m}}t}}{2} = \sin h\sqrt{\frac{\beta^2+4km}{2m}}t$ and then finally, we write the equation of motion as

$$r(t) = \frac{qEo}{k}\left\{1 - e^{\frac{-\beta t}{2m}}\left[\cos h\left(\sqrt{\frac{\beta^2+4km}{2m}}t\right) + \frac{\beta}{\sqrt{\beta^2+4km}}\sin h\left(\sqrt{\frac{\beta^2+4km}{2m}}\ t\right)\right]\right\} \quad 4.18$$

Equation 4.18 is solution of the equation of motion of the cell obtained from the resultant forces acting on the cell as it was trapping. So that just before the cells were entering the laser trap, they were at rest. We use nonlinear model fit in Wolfram Mathematica 12.1 to determine the charge (q) and the trapping constant (spring constant), k from the theoretical model of Equ.4.18 and the measured displacement versus time data for individual cell. From the nonlinear model, the fit function started looking for the charge (q) and coefficient of the trap (k), where the mass of the individual cells, the drag coefficient (β), and the electric field (Eo) were known. Equation (4.8) is the equation of a damped harmonic oscillator with electrically driving force. In our experiment, the momentum of the cell increases when it moves towards the laser trap, while it decreases nearer to the center of the laser trap. Thus, the motion of the cell must be under damping, electrically driven harmonic oscillator. This necessitates that the solution in equation (4.18) continue to be hyperbolic and not trigonometric. The measured k value ranges from $0.05\mu\frac{N}{m}$ to $1.11\mu N/m$ with average values $0.38\mu N/m \pm 0.09\mu N/m$.There were small differences in the trapping coefficient

of k in each 24-hour-treated breast cancer cells. Table 4.2 shows that there is some difference between the average trapping coefficient that was measured and the trapping coefficient of the individual cells. As previously stated, k is proportional to the cells polarization. Polarization is determined by the area of the cell and the polarizing electric field. Equation 4.18 found that the unknown variables: the charge on the breast cancer cells (q) and the trapping coefficient (spring constant) k, with a confidence interval of 0.5μN/m. All 27 of the breast cancer cells that were given a 24-hour treatment had extremely high determination agreement values (R^2), with the lowest agreement value being 0.9954. The value of the charge developed and the coefficient of the laser trap for each 24-hour treatment of breast cancer cells are different. Given that both k and q were fitted simultaneously, it is possible that k's fitting had an impact on q's value. Table 4.2 shows that the magnitude of charge developed in Z, the coefficient of the trap, radius, diameter, and the minimum and maximum R^2 value of the 27 pre-ionized, 24-hour-treated breast cancer cells.

	24 hour treated breast cancer (27)				
Quantities	Mean	Standard deviation	Min	Median	Max
Charge in Z	2249.5	5395.67019	10.50456	175.1074	18096.19
Coefficient ofthe trap(K) (μN/m)	0.375228	0.242987	0.0519569	0.34002	1.1024
Nlm[R^2]			0.9954		0.999985
Radius before(μm)	7.16373	1.28238	4.94485	6.98097	10.0351
Diameter before(μm)	14.3275	2.56476	9.88971	13.961	20.0703

Table 4.2 the magnitude of charge developed in Z, the coefficient of the trap, radius before, diameter before, and the minimum and maximum R^2 value of the 27 pre-ionized, 24-hour-treated breast cancer cells.

As before described, the nonlinear model fit function was used to find the unknown constants which are, the trapping coefficient and the charge developed on each 24-hour-treated breast cancer cell. The amount of charge developed on each of the 27 pre-ionized cell is expressed in terms of the magnitude of the charge of an electron or Z number ($Z = \frac{q}{e} = \frac{q}{1.602\times10^{-19}C}$). The average Z number for the pre-ionized, 24-hour-treated breast cancer cells is 2249.55 $\pm$1983.89. The large standard deviation in the charge could result from dissimilarities in cell sizes. The size of the cells before they are ionized ranges from 4.94µm to 10.00µm, with an average diameter of 14.3µm$\pm$0.94µm as we have seen from table 4.2

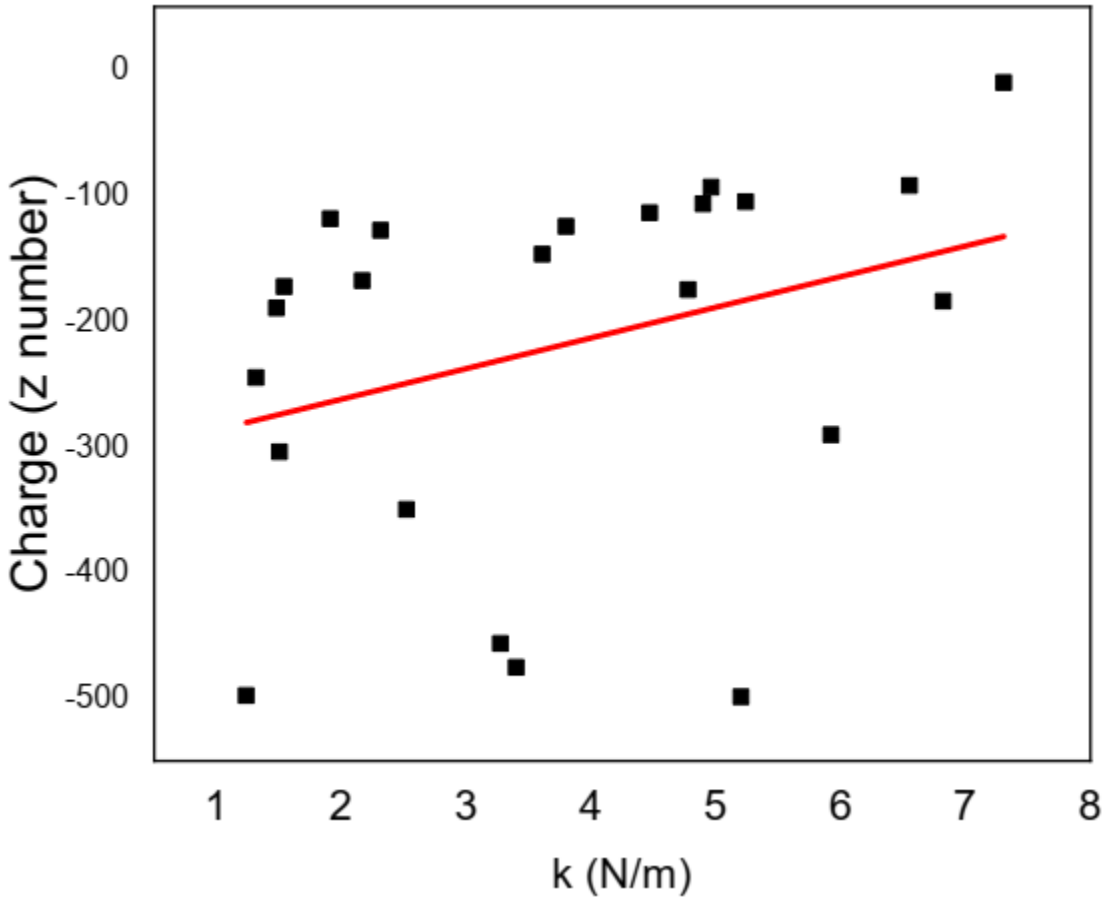

Figure 4.4shows the charge versus the spring constant of the cells

The graph 4.4 represents the data analysis related to the charge development and spring constant of pre-ionized breast cancer cells. From your description, it appears that Figure 4.4 shows a scatter plot and the linear fitting by a red line graph representing the relationship between the charge development on pre-ionized breast cancer cells and their spring constant. The graph indicates that there is a linear or direct correlation between these two variables, as depicted by the red line.

Based on the information provided, it is also mentioned that the size of the cells and the charge developed on the cells have a positive relationship. Larger cells tend to develop more electric charges, while smaller cells develop smaller charges. Additionally, you mentioned that the spring constants of the pre-ionized breast cancer cells also depend on the size of the cells. Using origin pro2019b software, the displacement vs. time data for each 24 hourly treated breast cancer cell was derivate; this results in the velocity.

Figure (4.5) shows the velocity time graph for 27 pre-ionized, 24-hour-treated breast cancer cells.

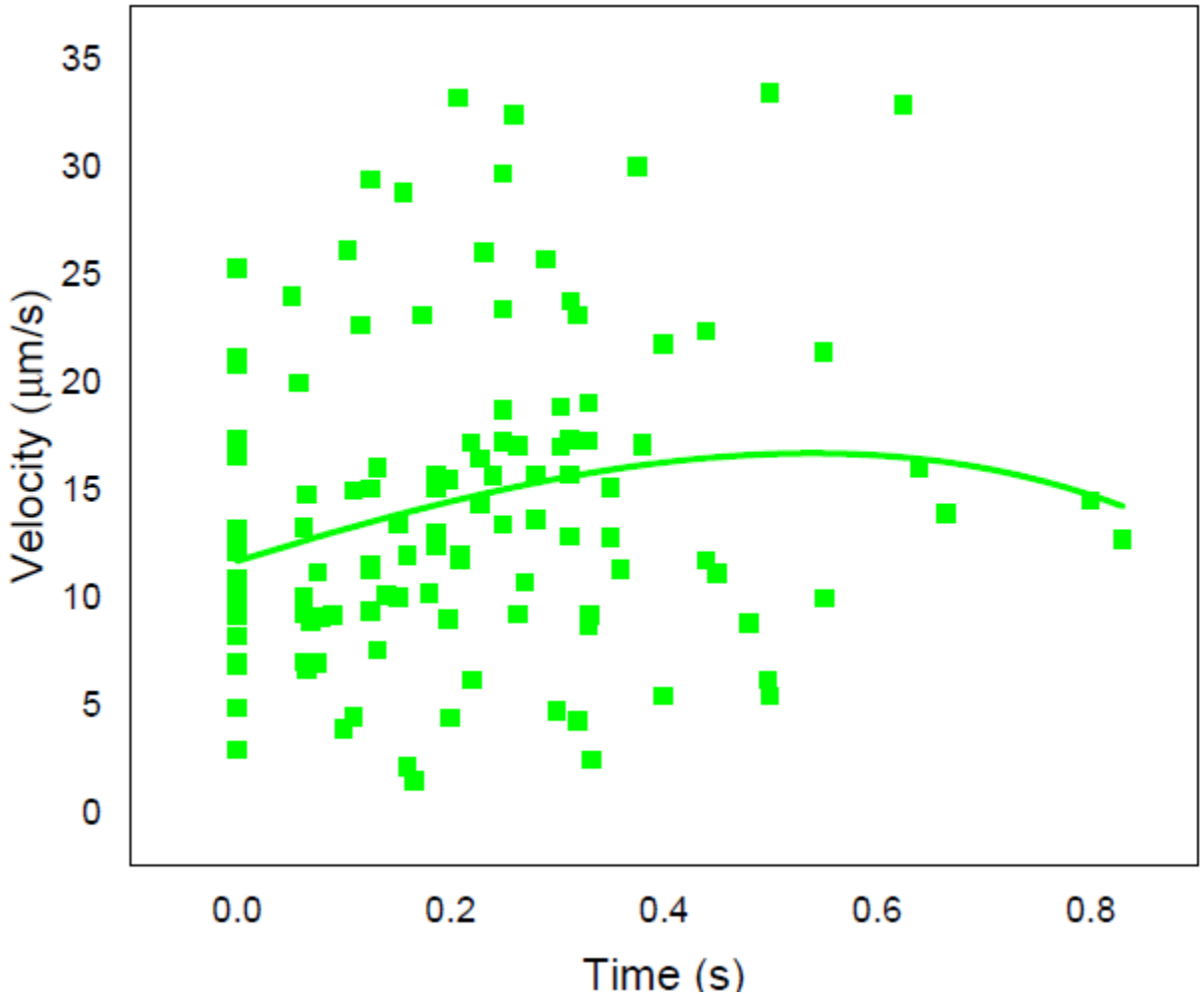

Figure 4.5 Velocity vs. time graph for pre-ionized, 24-hour-treated breast cancer cells

Figure (4.5) shows that the velocity of the cells increases to some extent when they are moving towards the trap. While close to the center of the laser trap, their velocities decrease. This is due to the electrostatic force and the force due to electric field since near the trap stronger polarization charge is induced. And also, near to the center of the laser trap, more charges develop on the cells,

and the electrostatic forces increase. This field force pushes back the cells, and their velocities decline, as shown in the graph from t = 0.3 to 0.8 s.

In our experiment, we observed that all cells possess a negative charge on their surface, but our objective was to deal with the magnitudes; the charges were expressed in z numbers. Figure 4.6 illustrates the charge in z vs. the average velocity of the pre-ionized, 24-hour-treated breast cancer cells.

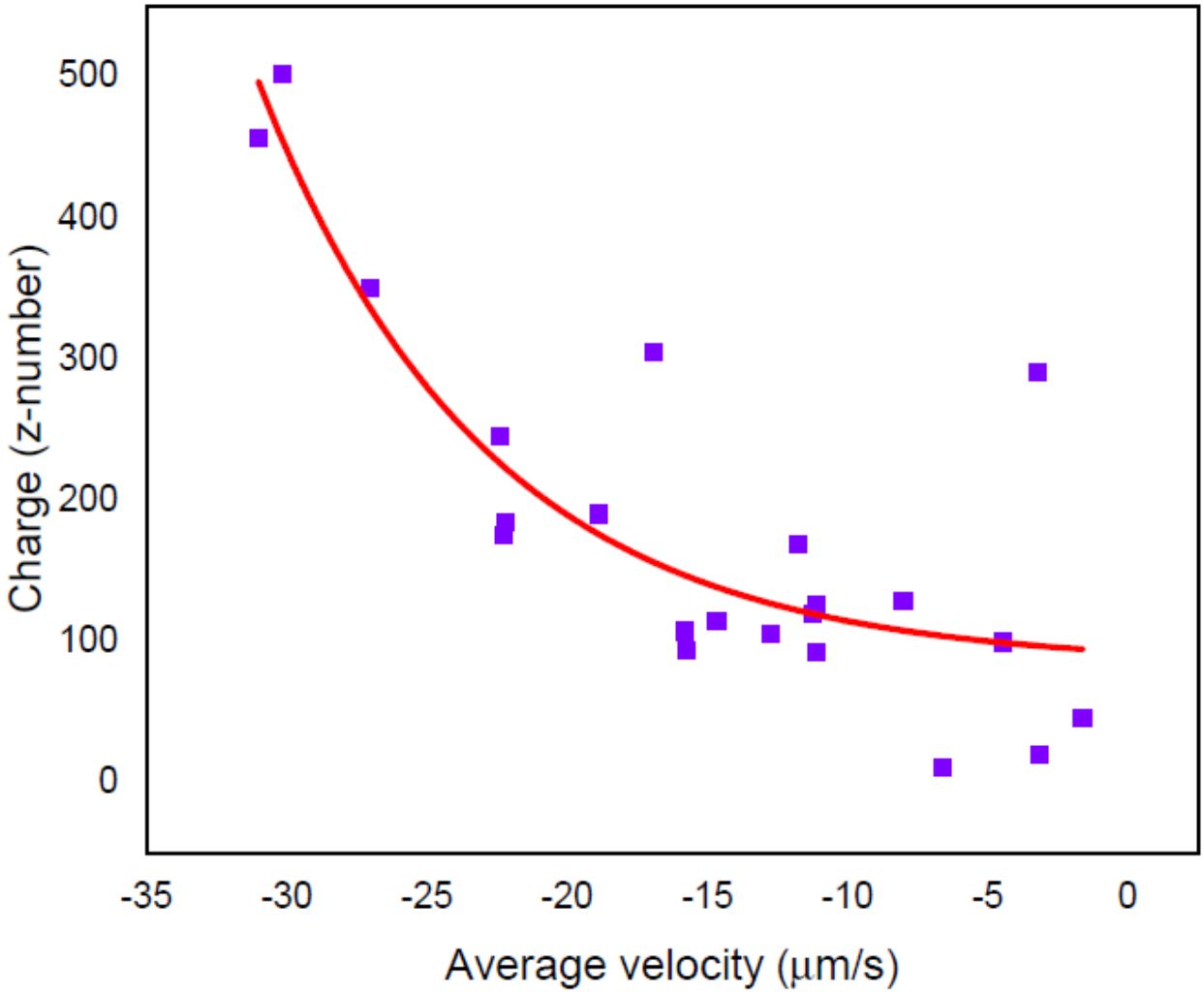

Figure 4.6 Charge (Z) vs. average velocity of the 24-hourly treated breast cancer cells.

When the breast cancer cells move into the trap, a charge develops on the cells, and their velocities are inversely proportional to each other as shown on the graph. This could happens due to

Coulomb force. The strong electric field breaks up dipole oscillations that accumulate free charge on the cells, and the Coulomb force opposes the trapping force. Further more information the charge develops on the cell increases their velocity decreases. Like the velocity, the acceleration of each cell was calculated by the second derivative of the displacement vs. time data using the origin Pro2019b software. Figure (4.7) shows the acceleration vs. time graph for pre-ionized, 24-hour-treated breast cancer cells.

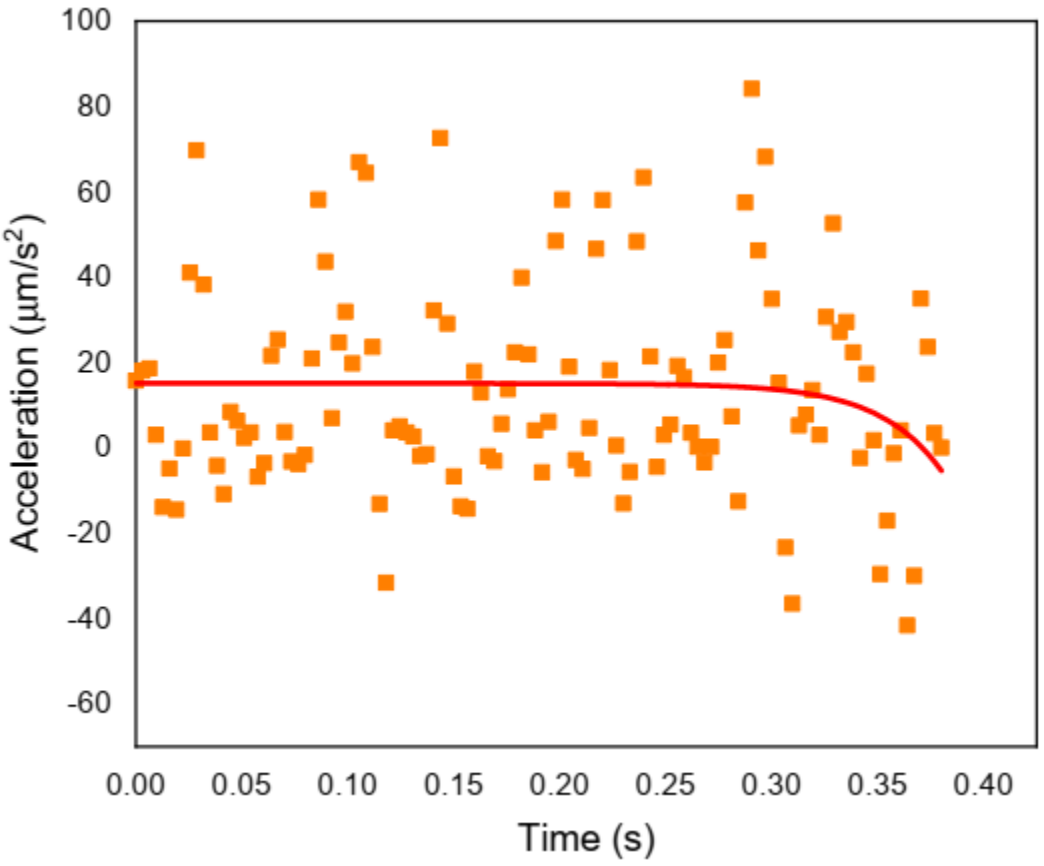

Figure 4.7 the acceleration vs. time graph for 27 pre-ionized, 24-hour-treated breast cancer cells

The fig.4.7 shows the dynamics of the cells when they are moving to the trap and they have constant acceleration from t=0 to t= 0.3 s. when the cells approaching to the center of the trap, they start to decelerate until they were trapped. The decreasing acceleration were due to strong polarization and breakdown dipole-dipole interaction which increase number of free charges on the surface of the cells. This tells us ionization of the cells start before they inter to the trap because the cells develop more charges. As a result, the electrostatic force and the induced field are stronger. This force pushes the cells out of the trap, and the acceleration of the cells decelerate.

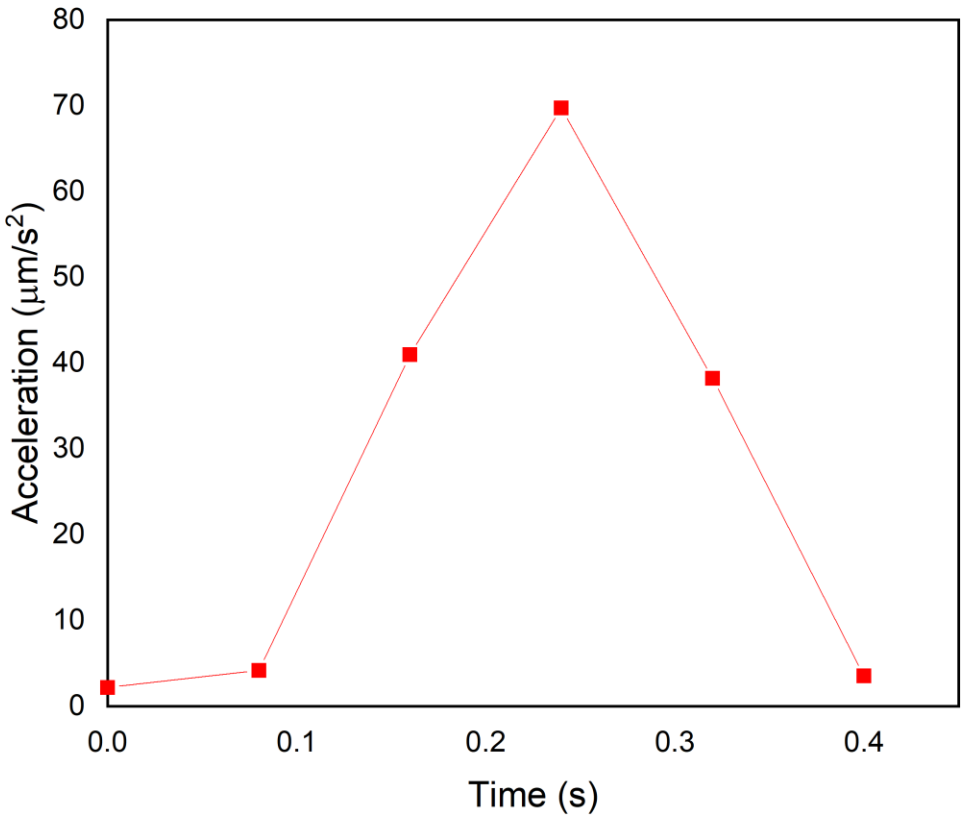

Figure4.8 acceleration vs time graph

Figure 4.8 shows the acceleration of single cell. The acceleration increases from 0 m/se^2 to 70 m/se^2 and decreases from 70 m/se^2 to 0 m/se^2. Because the charge developed on the cell increases when the cell moves toward the laser trap. However, near the center of the laser trap, the electrostatic force is greater than the trapping force. Due to this, the cells are decelerating and pushing back from the center of the laser trap.

CHAPTER – FIVE

5. CONCLUSION AND RECOMMENDATION

5.1 CONCLUSION

This section will serve as a recapitulation, highlight reel, and discussion of the major topics of the studies. The electrical characteristics of breast cancer cells that had been pre-ionized and treated for 24 hours with the anti-tumor agents 2-Dodecyl-6-methaxycyclohexa-2, 5-diene-1, 4-dione (DMDD) were investigated in our work on 4T1 breast cancer cells. The charge and laser trap coefficient were determined. This was done by forming the equation of motions of the pre-ionized cells with Newtonian mechanics. The net force performing on the cell as it enters the laser trap was used to find the equation of motion for cancer cells. These forces are the electrostatic force, the laser trap force, and the drag force. The in homogenous second order differential equation was solved after the determination of electro static force and trapping force. Using mass, electric field, and drag coefficient, the theoretical model was evaluated for each breast cancer cell. By applying a numerical nonlinear model fit function, it was possible to determine the charge that developed on the cells and the laser trap coefficient, particularly for each cell. The average measured value of charges and their trap coefficient was 2249.55 units and $0.38 N/m$ respectively. Cell diameter and charge development on the cells are directly proportional, indicating larger cells have more charges .The strength of induced electric field increase as the cell approaches to the trap and also the oscillation of the dipole moment increase. Polarization depends on the area of the cell and the polarizing electric field. The momentum of the cells and electric charges increases as they move into the laser trap while momentum decrease close to the center of the laser trap. The acceleration and velocity of the pre-ionized cells were obtained by taking the derivatives of displacement versus time data by using the Origin Pro 2019 b software. Acceleration decreases near to in the laser trap. When the cells trapped to a laser the velocity of the cells and the charge develops on their surface have a negative relation ships

5.2 RECOMMENDATION

In this study, the electric charge developed on each 24-hourly treated breast cancer cell and the coefficient of the laser trap were measured. During this study, the age of the cells and the amount of time they had spent outside of the incubator were not taken into account, and the negative and

positive impact of temperature on the cells after incubation were not considered. Because it may have a factor on the value of the charge and coefficient of the laser trap of the cells. We recommend developing the research line as above.

REFERENCES

1. EBERLY, P. W. J., 2010. *Laser physics.* canda : JOHN WILEY&SONS,INC.,Hoboken New Jergey pupulished simultaneously in canda
2. BENGLAND, S., 1988. Introduction toMid Laser therapy. *IEEE Journal of quntum electronics,26(12),* p. 1.

3. E. muhammed, "Chemo treated 4T1 breast cancercells radation response measured by single and multipel cellionization using infrared laser thrarpy," *chemo trated 4T1 breast cancer,* pp. 1-3, 2019.
4. Robert E.Mansel, O. F. a. W. G., 2007. *metastasisof breast cancer.* Nether land : springe
5. Ali Ashkbar1, F. R. A. S. A., 2020. Tretement of breast cancer in vivo by dual photodynamic and photothermal approches with the aid of our cumin photosensitizer and magnatic nano particles. *Nature reserch* , p. 1
6. TOMOHIKO OBAYASHI 1, K. F. (2015). Tretment with near-infrared radation promotes opoptosis inpancratic cancer cells. *DOI:10.3892/012015.3399,* 1.
7. E. muhammed, "Chemo trated 4T1 brast cancer cells radation respons measured by single and multiple cell ionization using infrared laser therapy," *chmo treated 4T1 breast cancer (2019)9:17547/https:// doi:.or/10.1038/541-598-019-53821/,* pp. 1-3, 2019.
8. Harvey Lodish, A. B. (2008). *molecular cell biology* .
9. E. muhammed, "Chemo trated 4T1 brast cancer cells radation respons measured by single and multiple cell ionization using infrared laser therapy," *chmo treated 4T1 breast cancer (2019)9:17547/https:// doi:.or/10.1038/541-598-019-53821/,* pp. 8, 2019.
10. Baskar, R. (2012). Cancer and radation therapy :current advinces and future directions . *international Journal of medical science* .
11. S. G. A. S. H. S. a. A. I. Amit Sengupta1*, "Effect of Low Frequency Electrical Current on the Biophysical and molecular properties of cancer cells," *International Journal ofcancer and clinicalResearch,* vol. 8, no. 1, p. 1, 2021
12. M. K. Siegel RL, "Cancer statics, 2022," CA: A cancer journal for clinicians2022, no. last acceded may 10, 2022, pp. 72(1):7-33, 2022.
13. sosity, A. c. (2019). *Breast cancer facts and figures 2019-2020.* America : American cancer sosity
14. E. muhammed, "Chemo trated 4T1 brast cancer cells radation respons measured by single and multiple cell ionization using infrared laser therapy," *chmo treated 4T1 breast cancer (2019)9:17547/https:// doi:.or/10.1038/541-598-019-53821/,* pp.9 , 2019
15. socity, A. c. (November 19, 2021). *Breast Cancer Basics.* amercan cancer socity.

16. by Breast Cancer Now's clinical specialists, a. b. (Breast Cancer Now, July 2021, BCC17). *CHEMOTHERAPY*. London: Breast Cancer Now.

17. American cancer socity, c. |. (October 27, 2021). *Treating Breast Cancer.* American cancer socity

18. L.Sampaio, K. a. (2011). *Memrane organazation and lipid rafts.* Germany: Cold sprin Harbor Laboratory press.

19. Marc Eeman, M. D. (2009). *From biological membranes to biomimetic model membranes* . Gembloux(Beligium): BASE

20. E. muhammed, "Chemo trated 4T1 brast cancer cells radation respons measured by single and multiple cell ionization using infrared laser therapy," *chmo treated 4T1 breast cancer (2019)9:17547/https:// doi:.or/10.1038/541-598-019-53821/,* pp.13-14 , 2019

21. DANA GAuS{KOVAu 1*, B. B. (Yeast 14, 1189–1197 (1998)). Fluorescent Probing of Membrane Potential in WalledCells: diS-C3(3) Assay in Saccharomyces cerevisiae. 1.

22. Moustafa, S. (2014). The electrical property of cancer cells. 4-17.

23. Mohammed, E. (2019). Application of laser trapping to study the Radio-sensitivity of. *Chemo treated 4T1 breast cancer cells,14*

24. Mohammed AliAnsari, E. M. (2011). Mechanisn of laser tissu intraction:opotical propertiy of tissue. *Journal of lasers in medical scienc .volume 2,number3*, 2.

25. TOMOHIKO OBAYASHI 1, K. F. (2015). Tretment with near-infrared radation promotes opoptosis inpancratic cancer cells. *DOI:10.3892/012015.3399*, 1.

26. Borja Mercadal1, P. T. (n.d.). Dependence of electroporation detection threshold on cell radius: an 1 explanation to observations non compatible with Schwan's equation 2 model. *Frank Reidy Research Center for Bioelectrics*, 2-3.

27. E. muhammed, "Chemo trated 4T1 brast cancer cells radation respons measured by single and multiple cell ionization using infrared laser therapy," *chmo treated 4T1 breast cancer (2019)9:17547/https:// doi:.or/10.1038/541-598-019-53821/,* pp. 16, 2019

28. Borja Mercadal1, P. T. (n.d.). Dependence of electroporation detection threshold on cell radius: an 1 explanation to observations non compatible with Schwan's equation 2 model. *Frank Reidy Research Center for Bioelectrics*, 2-3

29. R. Benz, F. B. (February 1979). *Reversible Electrical Breakdown.* Springer-Verlag New York Inc
30. E. muhammed, "Chemo trated 4T1 brast cancer cells radation respons measured by single and multiple cell ionization using infrared laser therapy," *chmo treated 4T1 breast cancer (2019)9:17547/https:// doi:.or/10.1038/541-598-019-53821/,* pp. 18, 2019
31. Ashkin, A. (1992). Forces of a single-beam gradient laser trap on a dielectric sphere. *Biophysical Journal,Volume 61*, 1
32. WILLIAM H. WRIGHT, G. J. (1990). Laser Trapping in Cell Biology. *IEEE JOURNAL OF QUANTUM ELECTRONICS, VOL. 26, NO. 12*, 2.
33. Mohammed, E. (2019). Application of laser trapping to study the Radio-sensitivity of. *Chemo treated 4T1 breast cancer cells,18-19*
34. Chunxia Chen1, Z. N. (2017). 2-Dodecyl-6-methoxy cylohexa-2,5-diene-1,4-dione in habits the growth and metastasis of breast carcinoma in mice. 1
35. Yohei Tanaka, 1. K. (2010). Non-thermal cytocidal effect of infrared irradiation. *the offfical journal of Japan cancer association* , 1.
36. Fei Yan 1, 3. W. (2016; 6(13):). NIR-Laser-Controlled Drug Release from DOX/IR-780- . *Theranostics*,1
37. Lúcio Frigo1, J. S. (2009). The effect of low-level laser irradiation (In-Ga-Al-AsP - 660 nm) on. *BMC Cancer*, 2-3.
38. Shaevitz, J. W. (August 22, 2006). *A Practical Guide to Optical Trapping.* University of Washington, Vol. 138.
39. Mohammed, E. (2019). Application of laser trapping to study the Radio-sensitivity of. *Chemo treated 4T1 breast cancer cells*
40. DIMITROV, D. (1995). Electroporation and electro fussion of membranes . In *Handbook of Biological Physics* (pp. 855-869). Elsevier Science B.V
41. E. muhammed, "Chemo trated 4T1 brast cancer cells radation respons measured by single and multiple cell ionization using infrared laser therapy," *chmo treated 4T1 breast cancer (2019)9:17547/https:// doi:.or/10.1038/541-598-019-53821/,* pp. 46, 2019